^{2}H NMR Study on Phase Transitions and Crystal Dynamics of *p*-Chloro- and *p*-Bromobenzyl Alcohols

Motohiro Mizuno, Masanori Hamada, Tomonori Ida, Masahiko Suhara, and Masao Hashimoto[a]

Department of Chemistry, Faculty of Science, Kanazawa University, Kanazawa 920-1192, Japan
[a] Department of Chemistry, Faculty of Science, Kobe University, Nadaku, Kobe 657-8501, Japan

Reprint requests to Dr. M. M.; E-mail: mizuno@wriron1.s.kanazawa-u.ac.jp

Z. Naturforsch. **57 a,** 388–394 (2002); received January 23, 2002

Presented at the XVIth International Symposium on Nuclear Quadrupole Interactions, Hiroshima, Japan, September 9-14, 2001.

Two phase transitions of 4-chlorobenzyl alcohol (*p*CBA) and 4-bromobenzyl alcohol (*p*BBA), from the low-temperature phase (LTP) to the intermediate-temperature phase (ITP) and from ITP to the room-temperature phase (RTP), were investigated by ^{2}H NMR and differential scanning calorimetry (DSC). The crystal dynamics in each phase were studied using the ^{2}H NMR spectra, the spin-lattice relaxation time (T_1) and the relaxation time of quadrupole order (T_{1Q}) for the samples, where the hydrogen of the -OH group was selectively deutrated. The ^{2}H NMR T_1 of both crystals in the RTP were dominated by the fluctuation of the electric field gradient at ^{2}H nucleus caused by vibrational motions of the -CH_2OH group. In the LTP of both crystals, the fast jump of hydrogen atoms between the two sites corresponding approximately to the positions of the hydroxyl hydrogen atoms in the RTP and LTP were found from ^{2}H NMR spectra. The results of T_1 and T_{1Q} in the LTP revealed that the jump of hydrogen atoms occurs in asymmetric potential wells and that these potential wells gradually approach symmetric ones with increasing temperature on the high-temperature side in the LTP.

Key words: Crystal Structure; Phase Transition; ^{2}H NMR; Crystal Dynamics; Hydrogen Bond.

Introduction

The title compounds, 4-chlorobenzyl alcohol (*p*CBA) and 4-bromobenzyl alcohol (*p*BBA) are known to undergo a first-order phase transition at T_{c1} = 236 and 217 K, respectively [1, 2]. Crystals of *p*CBA and *p*BBA are isomorphous (monoclinic, space group $P2_1$, Z = 2). The structure is characterized by the O-H···O hydrogen bonded chains along the 2_1 axis [3]. The results of ^{35}Cl, ^{85}Br NQR and dielectric measurements predicted another higher-order phase transition at T_{c2} = 218 and 195 K for *p*CBA and *p*BBA, respectively [1, 2]. These transitions should be closely related to the local structure of hydrogen bonds. ^{2}H NMR is a very powerful tool for investigating the dynamic structure in crystals. ^{2}H NMR spectra are useful for the determination of the motional mode, since the characteristic spectrum results from the molecular motion. The information of the rate and potential for the molecular motion can be obtained by the ^{2}H NMR spin-lattice relaxation time (T_1) and relaxation time of quadrupole order (T_{1Q}).

In the present work, the ^{2}H NMR spectra, T_1 and T_{1Q} were investigated in samples where the hydrogen of the -OH group was selectively deuterated, in order to study the dynamics of the O-H···O hydrogen bond network. Phase transitions were also examined by differential scanning calorimetry (DSC). We will discuss dynamic structures in each phase and mechanisms of these phase transitions.

Experimental

Preparation of Deuterated Compounds

Commercial compounds (nacalai tesque) of *p*-chlorobenzyl alcohol (*p*CBA) and *p*-bromobenzyl alcohol (*p*BCA) were recrystallized several times from suitable solvents to purify the materials. For the ^{2}H NMR experiment, the hydroxyl hydrogen in *p*CBA

was deuterated selectively by using D_2O in a dioxane solution to give *p*-Cl-C_6H_4-CH_2OD (abbreviated *p*CBA-d). By a similar method, *p*-Br-C_6H_4-CH_2OD (*p*BBA-d) was prepared. The degree of deuteration was checked by ^{1}H NMR of *p*CBA-d and *p*BBA-d dissolved in $CDCl_3$: no appreciable peak of ^{1}H NMR from the hydroxyl proton was found in the NMR spectrum of each compound.

Thermal Analysis

Thermal analysis of *p*CBA-d and *p*BBA-d was carried out by using differential scanning calorimeters (Rigaku DSC-8058 and Mac Science DSC 3100S).

^{2}H NMR

The ^{2}H NMR spectra were measured by using a CMX-300 spectrometer at 45.825 MHz. A $(\pi/2)_x$-τ-$(\pi/2)_y$-τ-acquisition pulse sequence was used. The $\pi/2$ pulse width and τ were 3.0 and 30 µs, respectively. T_1 was determined by the saturation-recovery and inversion-recovery methods. T_{1Q} was measured by the Jeener-Broekaert pulse sequence [4 - 6].

Results and Discussion

Phase Transitions

The thermal analysis on *p*BBA-d revealed a phase transition at (221 ± 1) K (T_{c1}) with an enthalpy of transition ($\Delta H(T_{c1})$) of ca. 1.0 kJmol^{-1}. This transition is of first-order, judging from the remarkable super-cooling observed for it. The T_{c1} in *p*BBA-d is higher than that in *p*BBA by ca. 4 K. The DSC curve of *p*BBA-d exhibited a small thermal anomaly at ca. 195 K. The small anomaly is considered to correspond to the higher-order phase transition reported for *p*BBA [2]. The thermal analysis of *p*CBA-d indicated a phase transition at (233 ± 1) K (T_{c1}), the onset of which was overlapped by a small thermal anomaly (exothermic drift) emerging from ca. 217 K. The value of T_{c1} in *p*CBA-d is lower than that in *p*CBA by ca. 3 K. The observed small anomaly is considered to correspond to the phase transition of *p*CBA found at ca. 218 K [2].

The temperature dependences of T_1 of ^{2}H NMR are shown in Figs. 1 and 2 for *p*BBA-d and *p*CBA-d, respectively. The jump of T_1 of *p*BBA-d at around its T_{c1} observed on heating can be assigned to a first-order phase transition. As can be seen in Fig. 1, a

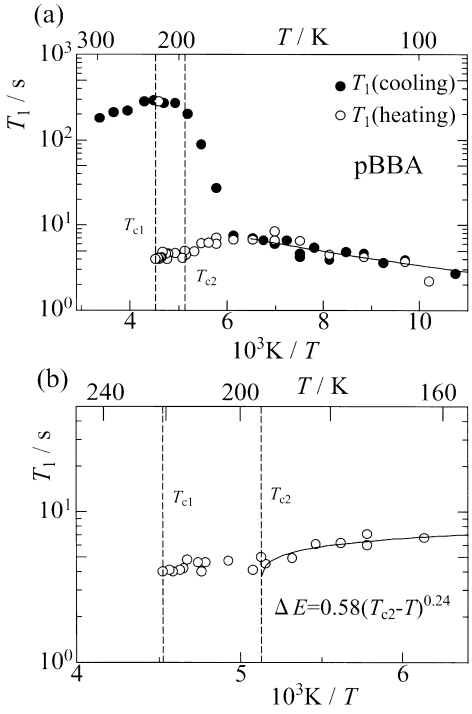

Fig. 1. Temperature dependence of ^{2}H NMR T_1 in *p*BBA. (a) T_1 in the heating and cooling processes. The solid line indicates the fitting curve by use of (3 - 5). (b) T_1 around the phase transition points in the heating process. The solid line indicates the fitting curve by use of (3 - 5), assuming $\Delta E = \alpha(T_{c2} - T)^{\gamma}$.

super-cooling of this transition was observed when the sample was cooled from room temperature. It took more than 8 hours until T_1 reached an equilibrium value at 180 K. On heating from 90 K, the $\log(T_1)$ vs. $1/T$ curve showed a break around 160 K, followed by a decrease of T_1 occurring between 170 and 195 K. At temperatures higher than 195 K, T_1 appeared to remain constant till the temperature reached T_{c1}. This anomalous behavior of the $\log(T_1)$ vs. $1/T$ curve seems to agree with the appearance of the small thermal anomaly at 195 K found for *p*BBA-d.

In the $\log(T_1)$ vs. $1/T$ curve of *p*CBA-d one can find a jump of T_1 assignable to a first-order phase transition of this compound at T_{c1}. As indicated in Fig. 2, a super-cooling of this transition appeared when the sample was cooled from room temperature. In the $\log(T_1)$ vs. $1/T$ curve, a break can be seen around 190 K. This observation is consistent with the thermal behavior mentioned above.

On the ground of the present thermal analysis and the observed T_1 vs. T relations, we could show

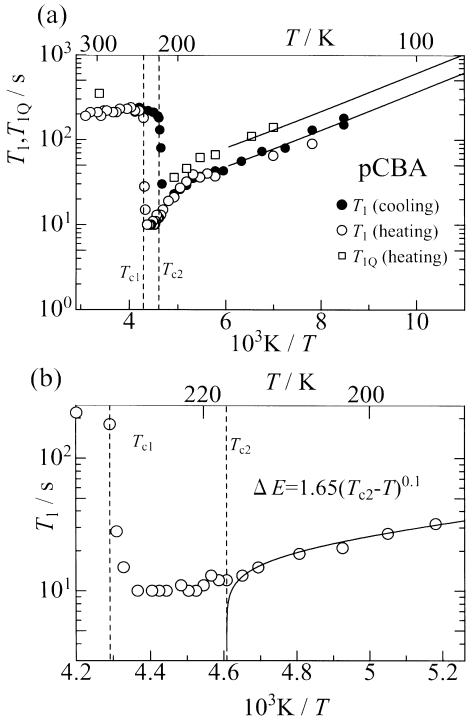

Fig. 2. Temperature dependences of ^{2}H NMR T_1 and T_{1Q} in *p*CBA. (a) T_1 and T_{1Q} in the heating and cooling processes. The solid line indicates the fitting curve by use of (3 - 6). (b) T_1 around the phase transition points in the heating process. The solid line indicates the fitting curve by use of (3 - 5), assuming $\Delta E = \alpha(T_{c2} - T)^{\gamma}$.

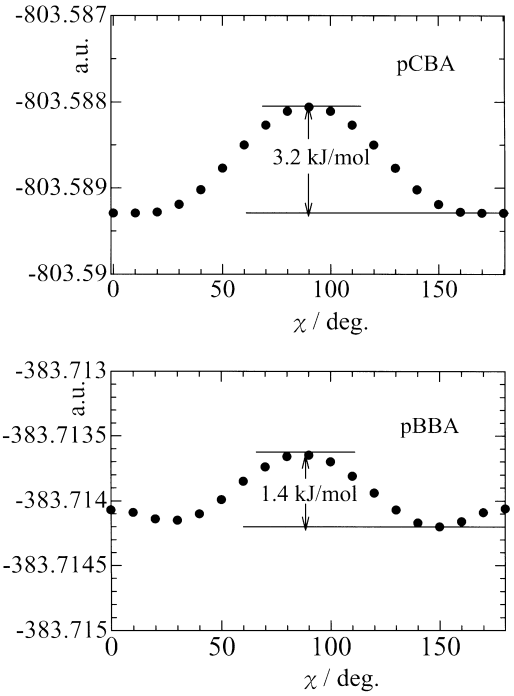

Fig. 3. Potential energies of *p*CBA and *p*BBA molecules as a function of the dihedral angle O1-C7-C1-C2 (χ).

the presence of two phase transitions in each compound, for *p*BBA-d transitions at 195 and 221 K, and for *p*CBA-d those at 217 and 233 K. The relevant phases will be referred to by RTP, ITP, and LTP, respectively, in the order of decreasing temperature.

Temperature Dependence of the Crystal Structure

Crystal structures of *p*CBA and *p*BBA have been studied at various temperatures in the range 130 < T /K < 300 [7].

The first order phase transition in *p*CBA was shown to be accompanied by a remarkable jump of the dihedral angle O1-C7-C1-C2 (χ) (for the atomic numbering scheme, see Scheme 1). On the other hand, it has been found that the orientation of the benzene ring is substantially independent of temperature, leading to the conclusion that the jump of χ can be attributed to a displacement of the oxygen atom.

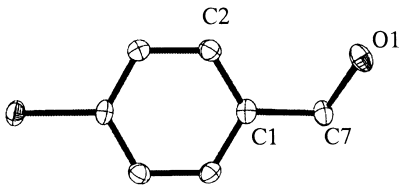

Scheme 1. Atomic numbering scheme.

Potential energies in *p*CBA and *p*BBA molecules for several χ values were estimated by an *ab initio* MO calculation using the GAUSSIAN 98 program [8]. The calculation was performed at Hartree-Fock level with the 6-311G(d,p) basis set. Figure 3 indicates plots of potential energy vs. χ for *p*CBA and *p*BBA. The gentle slope around the potential minimum reveals facility in the change of χ.

The intermolecular O···O distance in the hydrogen bond chain illustrated in Fig. 4 was found to show a slight discontinuity (ca. 0.01 Å) at the transition point. This observation indicates that the hydrogen bond chain shifts as a whole like a 'micro piston' along the crystal b axis when the phase transition takes place.

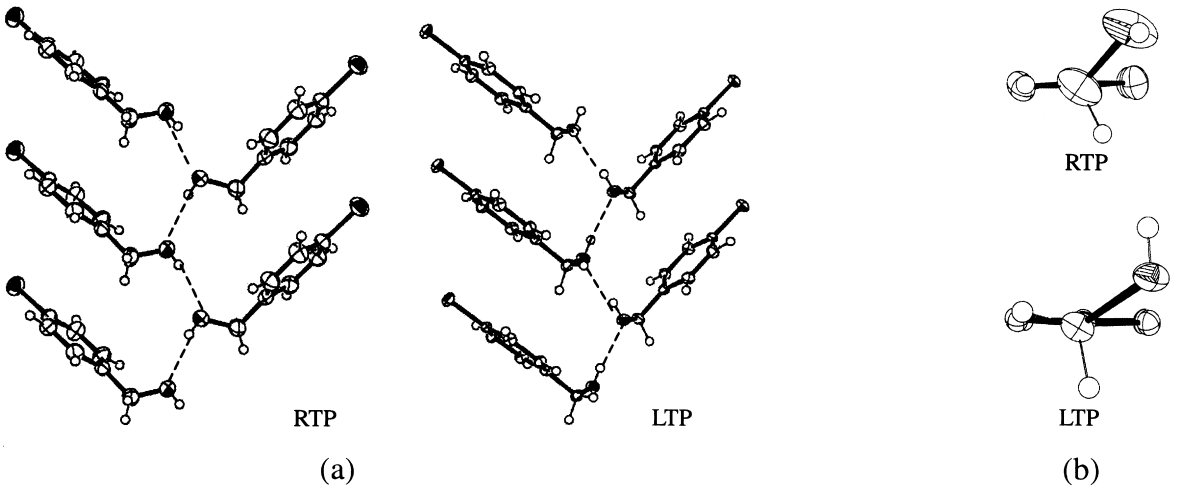

Fig. 4. (a) Hydrogen bonded chains of *p*CBA molecules in RTP and LTP. (b) ORTEP drawings of molecule in RTP and LTP.

As shown in Fig. 4, the direction of the hydrogen bond in RTP is opposite to that in LTP (and in ITP). It is also interesting that the hydroxyl hydrogen atom is located on *trans* position with respect to the benzene ring in RTP, while on *cis* in LTP and ITP. This conformational change seems to be favorable for the reversal of the direction of the hydrogen bond.

Similar phenomena are likely to occur also in crystals of *p*BBA [7].

Analyses of ^2H NMR

Figure 5 shows ^{2}H NMR spectra of *p*CBA-d and *p*BBA-d. The quadrupole coupling constant (e^2Qq/h) and asymmetric parameter (η) of both compounds were estimated from the ^{2}H NMR spectra as (210±2) kHz and 0.10 in LTP and (220±3) kHz and 0.05 in RTP, respectively.

The central peaks of the ^{2}H NMR spectra observed in the LTP and ITP indicates fast motion of the hydrogen and distribution of the hydrogen site in the hydrogen bond network. On the contrary, such a motion is absent in RTP, since the ^{2}H NMR spectra showed a typical Pake pattern.

In the RTP, T_1 of *p*CBA-d and *p*BBA-d amounts to a few hundred seconds and increases gradually with decreasing temperature. The crystal structure analysis of the RTP indicated that the thermal parameters of the oxygen and carbon atoms in the -CH_2OH group were larger than those of the other atoms [see, Fig. 4 (b)]. Therefore, T_1 in the RTP is considered to be dominated by the fluctuation of the electric field gradient at the ^{2}H nucleus caused by the vibrational motion of the -CH_2OH group.

The thermal parameters of these oxgen and carbon atoms were small below T_{c1}. Therefore, the ^{2}H NMR T_1 of *p*CBA-d and *p*BBA-d below T_{c1} are considered to be dominated by the local motion of the hydrogen in the H-bond network, such as the H-jump in the -OH group between the upward and downward orientations in the network.

On the low-temperature side in the LTP, the ^{2}H T_1 of *p*CBA-d decreased exponentially with increasing temperature, whereas T_1 of *p*BBA-d increased exponentially with increasing temperature.

The open square in Fig. 2 (a) shows the ^{2}H NMR T_{1Q} of *p*CBA-d in the heating process. A ratio T_1/T_{1Q} = 0.6±0.2 was obtained for *p*CBA-d in LTP. The ratio T_1/T_{1Q} becomes 1.5 in the limit of slow motion, and 0.6 in the limit of fast-motion [6]. Therefore, the relaxation of the ^{2}H nucleus is found to be in the fast motion regime.

The fact that T_1 of *p*CBA-d in the LTP decreases with increasing temperature seems to conflict with the fast motion regime, since T_1 increases with increasing temperature in the fast motion regime of the typical Bloembergen, Purcell, and Pound (BPP) theory [9]. However, this T_1 behavior in the LTP can be explained by the local motion of the H atom in the asymmetric potential wells shown in Fig. 6(a) [10, 11].

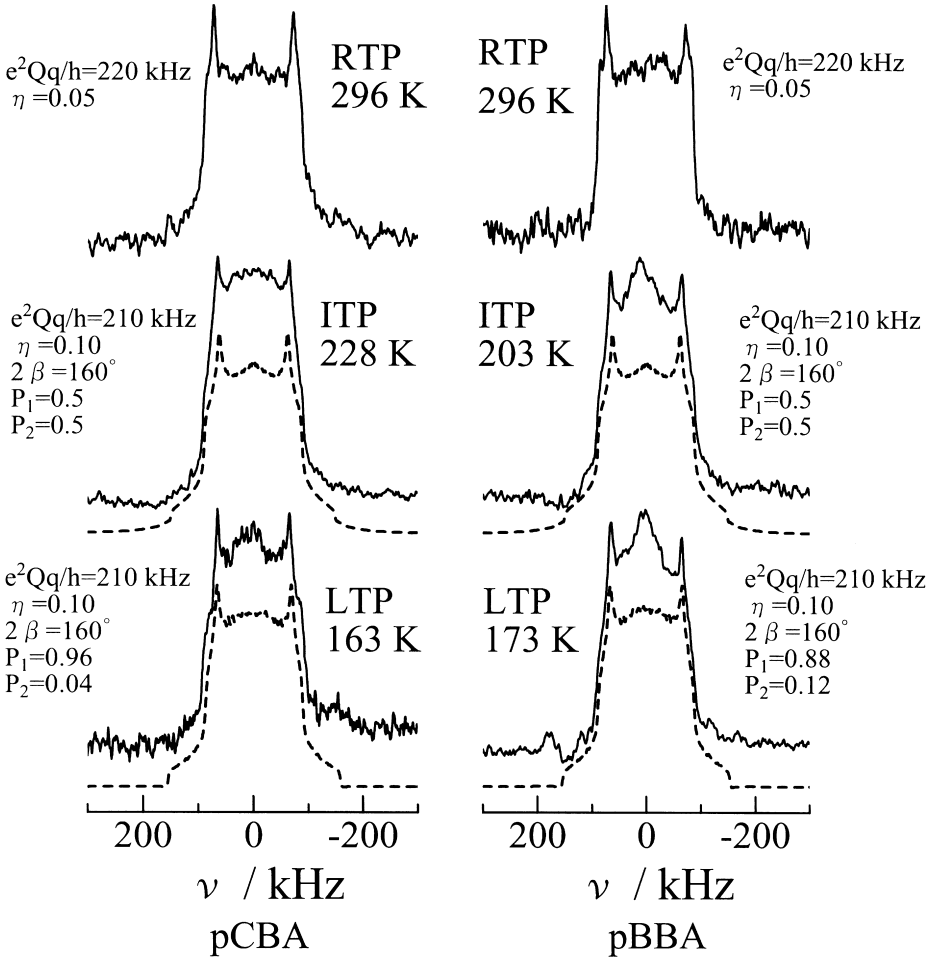

Fig. 5. ^{2}H NMR spectra for *p*CBA and *p*BBA. The broken lines show the simulated spectra.

For *p*BBA-d, an asymmetric potential can be applied for the local motion of hydrogen, since the slope of the $\log(T_1)$ vs. $(1/T)$ curve in the LTP is very gentle (the activation energy was estimated as 1.9 kJmol^{-1} from the slope of $\log(T_1)$ vs. $(1/T)$).

The potential for the local motion of hydrogen in the LTP of *p*CBA-d is expected to be more asymmetric than that of *p*BBA-d from the temperature dependences of T_1.

For *p*CBA-d, a decrease in T_1 was observed in the range $195 < T/\mathrm{K} < T_{c2}$. In the case of *p*BBA-d, a similar phenomenon occurred in the range $170 < T/\mathrm{K} < T_{c2}$. These observations suggest that ΔE gradually decreases and the asymmetric potential wells for the local hydrogen motion approach to the symmetric ones (Fig. 6(b)) with increasing temperature. Therefore, the transition at T_{c2} may be regarded as of an order-disorder type.

When the hydrogen jumps between the asymmetric double minimum positions, T_1 and T_{1Q} are expressed by neglecting the small η value of 0.1 as [5, 6, 10, 11]

$$T_1^{-1} = \frac{1}{10}\frac{4a}{(1+a)^2}\left(\frac{3e^2Qq}{4\hbar}\right)^2 (\sin 2\beta)^2 \cdot \left\{\frac{\tau_c}{1+\omega_0^2\tau_c^2} + \frac{4\tau_c}{1+4\omega_0^2\tau_c^2}\right\}, \quad (1)$$

$$T_{1Q}^{-1} = \frac{3}{10}\frac{4a}{(1+a)^2}\left(\frac{3e^2Qq}{4\hbar}\right)^2 (\sin 2\beta)^2 \frac{\tau_c}{1+\omega_0^2\tau_c^2}, \quad (2)$$

$$a = \exp\left(\frac{2\Delta E}{RT}\right), \quad (3)$$

$$\tau_c = (1+a)^{-1}\tau_{c0}\exp\left(\frac{E_a + \Delta E}{RT}\right), \quad (4)$$

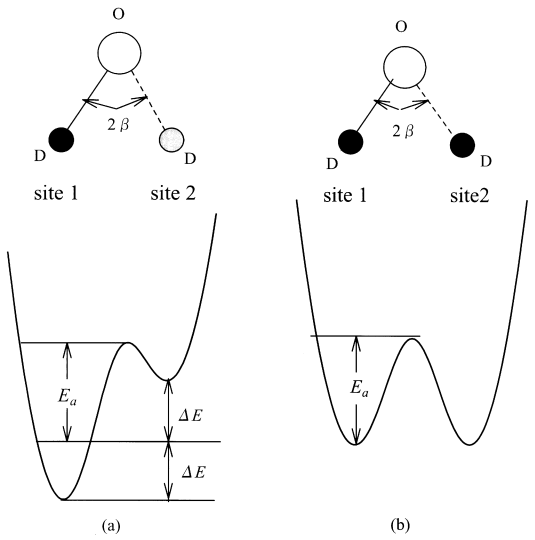

Fig. 6. Potentials for two-site jump of the hydrogen in the H-bond network; asymmetric (*left*) and symmetric (*right*) double minimum potential.

where 2β is the D-O···D angle, indicating separation between the sites 1 and 2 in Fig. 6(a). e^2Qq/h, ω_0, τ_{c0} and E_a are the quadrupole coupling constant, the angular NMR frequency, the correlation time at infinite temperature and the activation energy for the jump of the hydrogen of the -OH group, respectively. As can be seen from Fig. 6(a), ΔE indicates the deviation from symmetric potential wells. In the fast motion limit, $\omega_0\tau_c \ll 1$, (1) and (2) can be rewritten as

$$T_1^{-1} = \frac{1}{10}\frac{4a}{(1+a)^2}\left(\frac{3e^2Qq}{4\hbar}\right)^2 (\sin 2\beta)^2 5\tau_c, \quad (5)$$

$$T_{1Q}^{-1} = \frac{3}{10}\frac{4a}{(1+a)^2}\left(\frac{3e^2Qq}{4\hbar}\right)^2 (\sin 2\beta)^2 \tau_c. \quad (6)$$

By assuming $\Delta E = 0$ at T_{c2}, fitting calculations of T_1 and T_{1Q} below 190 K for *p*CBA and 160 K for *p*BBA were performed using (3 - 6). (E_a, ΔE), and $(3e^2Qq/4\hbar)^2(\sin 2\beta)^2\tau_{c0}$ were obtained as (2.5±0.2 kJmol^{-1}, 2.3±0.2 kJmol^{-1}), and 0.27 s^{-1} for *p*CBA-d and (5.4±0.3 kJmol^{-1}, 1.4±0.2 kJmol^{-1}), and 0.037 s^{-1} for *p*BBA-d.

By assuming the critical behavior of the form $\Delta E = \alpha(T_{c2} - T)^\gamma$, fitting calculations of T_1 in the ranges 195 < T/K < T_{c2} for *p*CBA-d and 170 < T/K < T_{c2} for *p*BBA-d was performed using (3 - 5) with E_a obtained for the LTP. The results of the fitting are shown in Figs. 1(b) and 2(b). For *p*CBA-d, the T_1 value at T_{c2} was evaluated as 3.6 s from the above model. However, the observed T_1 value (10 s) of *p*CBA-d at T_{c2} was larger than that. This discrepancy would come from the distribution of the correlation time due to the distribution of the local sites in *p*CBA-d. This is presumably caused by lattice defects, which has been confirmed by the ^{35}Cl NQR experiment for *p*CBA having the experience of the phase transition at T_{c1} [1].

By assuming a fast jump of hydrogen atoms between site 1 and site 2 in Fig. 6, ^{2}H NMR spectral simulations of *p*CBA-d and *p*BBA-d in LTP and ITP were performed using E_a and ΔE obtained by the analysis of T_1. e^2Qq/h = 210 kHz and η = 0.1, which were obtained from the ^{2}H NMR spectra in LTP, were used for the simulation. The populations of site 1 (P_1) and site 2 (P_2) in Fig. 6 were estimated from the relation $P_2/P_1 = \exp(-2\Delta E/RT)$. The broken lines in Fig. 5 show the simulated spectra. τ_{c0} was estimated as 2.4×10^{-12} and 3.2×10^{-13} s for *p*CBA and *p*BBA, respectively , from the ^{2}H NMR spectral simulation and the analysis of T_1.

From the ^{2}H NMR spectral simulation, 2β of the two compounds was estimated as (160±5)°. This 2β value seems reasonable, since the two sites, separated by 160°, correspond approximately to the positions of the hydroxyl hydrogen atoms in RTP and LTP.

The decrease in ΔE corresponds to the increase in the population of the site for the RTP and hence may be regarded as the initiation process of the phase transition from the ITP to the RTP.

Acknowledgements

The authors would like to express appreciation to Professor K. Yamamura of Kobe University and Professor T. Nakagawa of Darmstadt University of Technology for the preparations of *p*CBA-d and *p*BBA-d.

[1] H. Niki, K. Kano, and M. Hashimoto, Z. Naturforsch. **51a**, 731 (1996).
[2] M. Hashimoto, Y. Monobe, H. Terao, H. Niki, and K. Mano, Z. Naturforsch. **53a**, 436 (1998).
[3] M. Hashimoto and Y. Nakamura, Acta. Crystallogr. **C44**, 482 (1988).
[4] J. Jeener and P. Broekaert, Phys. Rev. **157**, 232 (1967).
[5] R. R.Vold and R. L. Vold, Adv. in Magnetic and Optical Resonance, Vol. 16, ed. by W. S. Warren, Academic Press, New York 1991.
[6] H. W. Spiess, J. Chem. Phys., **72**, 6755 (1980).
[7] M. Hashimoto et al, to be published.
[8] M. J. Frisch, G. W. Trucks, H. B. Schlegel, G. E. Scuseria, M. A. Robb, J. R. Cheeseman, V. G. Zakrzewski, J. A. Montgomery, (Jr.), R. E. Stratmann, J. C. Burant, S. Dapprich, J. M. Millam, A. D. Daniels, K. N. Kudin, M. C. Strain, O. Farkas, J. Tomasi, V. Barone, M. Cossi, R. Cammi, B. Mennucci, C. Pomelli, C. Adamo, S. Clifford, J. Ochterski, G. A. Petersson, P. Y. Ayala, Q. Cui, K. Morokuma, D. K. Malick, A. D. Rabuck, K. Raghavachari, J. B. Foresman, J. Cioslowski, J. V. Ortiz, B. B. Stefanov, G. Liu, A. Liashenko, P. Piskorz, I. Komaromi, R. Gomperts, R. L. Martin, D. J. Fox, T. Keith, M. A. Al-Laham, C. Y. Peng, A. Nanayakkara, C. Gonzalez, M. Challacombe, P. M. W. Gill, B. Johnson, W. Chen, M. W. Wong, J. L. Andres, C. Gonzalez, M. Head-Gordon, E. S. Replogle, and J. A. Pople, Gaussian 98, Gaussian, Inc., Pittsburgh, PA, 1998.
[9] N. Bloembergen, E. M. Purcell, and R. V. Pound, Phys. Rev. **73**, 679 (1948).
[10] K. Morimoto, K. Shimomura, and M. Yoshida, J. Phys. Soc. Japan **52**, 3927 (1983).
[11] M. Mizuno, Y. Hamada, T. Kitahara, and M. Suhara, J. Phys. Chem. A **103**, 4981 (1999).